

ENGINEERING OF SEMI-AUTOMATIC SEGMENTATION IN IMAGING FOR OSTEOPOROSIS

Abdulmuhssin Binhssan

SECURITY FORCES HOSPITAL, RIYADH, SAUDI ARABIA

Abstract: Osteoporosis is an illness that has an impact on bones, which exhibits a decrease in bone mass and a deterioration of the trabecular structures. Typically, the method used to detect it is bone densitometry, which measures the density of bones, which act in our body as a reservoir of calcium. However, it has been proven that it is possible to assist in the diagnosis of osteoporosis using radiological images by identifying and analyzing specific interest areas. The knowledge that medical professionals have allows the location of these areas within the images. However, it is very beneficial to have efficient and effective computer tools for detecting them, since the time that this process takes them can be excessive for large volumes of data. This work proposes a tool that allows, among other things, to detect in a semi-automatic way the regions of interest in the head of the femur bone and then apply assistance methods to the diagnosis of osteoporosis.

Keywords: Osteoporosis, bones, radiology, segmentation.

I. INTRODUCTION

The field of medical images involves the set of techniques and processes used to obtain images of different parts of the human body for clinical purposes either for diagnostic or pedagogical purposes [1]. The use of images in medicine is constantly growing, not only as a diagnostic method but also in the planning of treatments based on image-guided intervention procedures, minimal invasive surgery, and monitoring of patients undergoing drug treatment. There are numerous technologies to acquire medical images: X-rays, computed tomography (CT), ultrasound or ultrasound among the most known. Due to the equipment and capture protocols, it is usual to obtain an image containing a portion of the human body that in turn contains the objects of interest. Currently, and as a result of technological advances in medicine, numerous applications of digital medical image processing have been developed [2]. Osteoporosis is a skeletal disease characterized by a significant decrease in bone mass and deterioration of bone microarchitecture, which increases the risk of spontaneous fractures or minor trauma. The early diagnosis of osteoporosis allows increasing the effectiveness of corrective treatments. The most commonly used method to diagnose this disease is through bone mineral densitometry, which measures bone mass (BM). The loss of OM is an important factor in determining the probability that bones have to fracture. However, some researchers warn that the mineral density value cannot completely predict the risk of osteoporotic fractures. This is mainly due to the fact that the aforementioned parameter does not include information on the bone microarchitecture, which is seriously affected during the progression of the disease and is considered an important factor in the determination of fracture risk. Combining the measurement of bone mineral density with an evaluation of the characteristics of the microarchitecture increases the probability of making a correct diagnosis. In recent years, numerous studies have been carried out with the aim of characterizing the trabecular structure by means of texture analysis on simple radiographic images of different bone pieces, without the need for complex studies of computed tomography or magnetic resonance imaging [3].

When working with radiological images and more specifically in the diagnosis of osteoporosis, although the knowledge on the part of the doctors allows locating the objects of interest within them, this process can take a considerable time that can be counterproductive when they should be analysed large number of images [4]. That is why the need arises to develop new automatic or semi-automatic algorithms that accelerate this process of localization of regions of interest, to facilitate the use of diagnostic assistance tools by physicians. This paper presents an alternative that, using a series of image processing algorithms, allows semi-automatic detection of regions of interest in radiographic images in order to assist medical professionals in the diagnosis of osteoporosis.

II. IMAGING OF OSTEOPOROSIS

Osteoporosis is still most frequently diagnosed with conventional radiography, with the main radiographic features of systemic osteoporosis being increased radiolucency and cortical thinning [5]. Nevertheless, this technique is relatively subjective and has low specificity, as radiological signs can be depicted in advanced stages, when already a significant

amount of bone is loss (around 30%) [5]. It is therefore mandatory to evaluate bone in early stages of the disease, with densitometric techniques being capable to evaluate even subtle variation in BMD. In fact, BMD, which can be easily measured in clinical practice, accounts for about 70% of the various factors that affect bone strength. The goal of measuring BMD is not only to diagnose osteoporosis additionally to determine the likelihood of fractures occurring and to keep track of patients receiving pharmacological treatment [6]. BMD, or bone mass density, is a measurement of the quantity of bone in the body and can be conveyed as areal density (bone mass per unit region, expressed in g/cm^2) or volumetric density (bone mass per thickness area, expressed in g/cm^3) [1]. In vivo measurements of BMD can be obtained using a variety of densitometric methods, including DXA, quantitative CT (QCT), and numerical ultrasound (QUS) [6,7]. It is crucial to remember that, regardless of the specific BMD value, the medical diagnosis of osteoporosis initially depends on the occurrence of any major fragility fracture (such as a vertebral, hip, or wrist fracture). In actuality, only 39% of people with vertebral fractures had osteoporosis determined by DXA at the vertebral column, and only 25 percent by DXA of the entire hip [8].

Figure 1 is a collection of so-called scanning electron micrographs taken from biopsies of a healthy person and an individual with osteoporosis. The pattern of strong interconnected bone plates can be seen in normal bone. Osteoporosis causes the loss of a large portion of this bone, and the rest of the bone has a weaker rod-like structure. Additionally, a few of the rods are totally broken off. These isolated pieces of bone may be counted as mass of bone, but they have no bearing on bone strength.

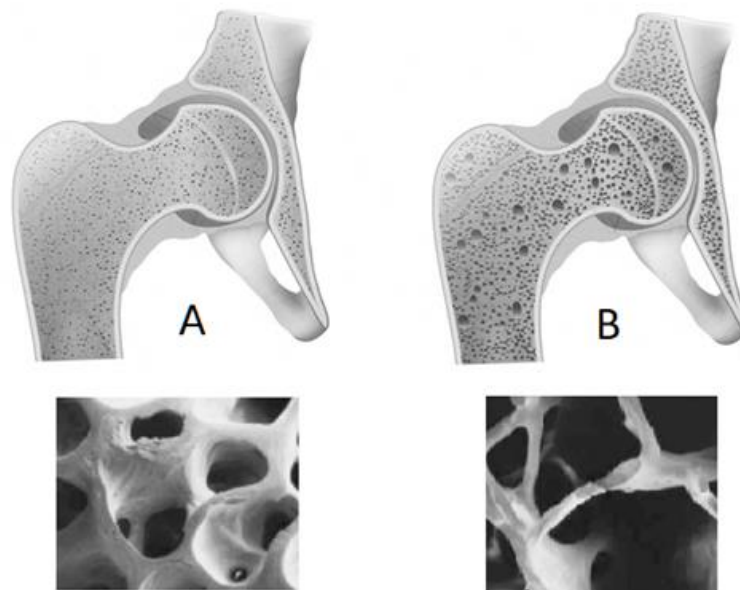


Fig.1 Bone in 2 conditions: Normal (A) vs Osteoporotic (B) [9].

In both clinical settings and academic research, DXA has become the most frequently used numerical bone imaging method for BMD indicators [10]. The areal BMD measurements provided by this quantitative method are expressed in grams per square centimeter (g/cm^2), which is well-known to be a significant predictor of bone strength and to be correlated with fracture risk (1).

The first benefit of DXA is its extremely low dose to patients, which ranges from 1 to 6 Sv and is regarded as insignificant when compared to background radiation from the environment (2.4 mSv) [11,12]. Second, measurements at these locations are the best for predicting the likelihood of fracture [19]. Examples of these locations include the proximal femur and the lumbar spine, which are particularly relevant to osteoporotic fractures. With an average coefficient of variability (CoV) ranging from 1% at the lumbar spine to 2% at the femoral neck, BMD measurements are extremely repeatable [10,14,15]. Finally, DXA scans are readily accessible and take only 1-3 minutes to complete.

However, DXA measurements of areal BMD also have some limitations because they are affected by changes in the density of the lumbar spine brought on by osteoarthritis or previous fractures, which may be prevalent among the elderly and typically lead to higher BMD values [5,16]. Additionally, because areal BMD measurements are size-dependent, they overestimate BMD in large bones and underestimate it in small ones, a flaw that can be problematic, particularly in young children [17,18].

The operator must focus on a number of factors, including patient demographic data, patient positioning, and scan analysis, in order to obtain a proper DXA scan. It has been demonstrated that DXA excellence is frequently impacted by errors in data collection, analysis, and interpretation, which may result in ineffective clinical decisions and diagnoses [16].

The pre-analysis image-cropping technique chose the side of the hip that was DXA-measured as the cropped side. As shown in Figure 2, the range cropped with the DXA measurement, the lines of the femur head and the underside of the lesser trochanter were chosen and included. The cropped area mimicked the osteoporosis evaluation range discovered by DXA. The images were cropped and then saved in PNG format. The BMD status of the patient wasn't disclosed to any of the orthopaedic specialists who did the cropping.



Fig.2 Hip radiograph prior to evaluation, with cropped region of interest

III. PROPOSED METHODOLOGY

For the detection of osteoporosis through X-ray images in the hip area, the trabecular texture should be found and analysed in what is known as the Ward triangle (TW) and the Main Compression Group (GCP). As shown in Figure 3, the TW is located in the area of the neck of the femur.

This area is located between the three trabecular bundles of the head of the femur and is the first place where the presence of osteoporosis begins to manifest, while the GCP is the last to see its structure modified [19]. In this way, a parameter obtained by comparing the texture of said femoral regions can give rise to an interesting descriptor of the degree of advancement of the disease, which, depending on the comparison of two regions within the same plate, would be free from the influence of the conditions of obtaining the radiography. The steps followed in the proposed tool will be briefly described below.

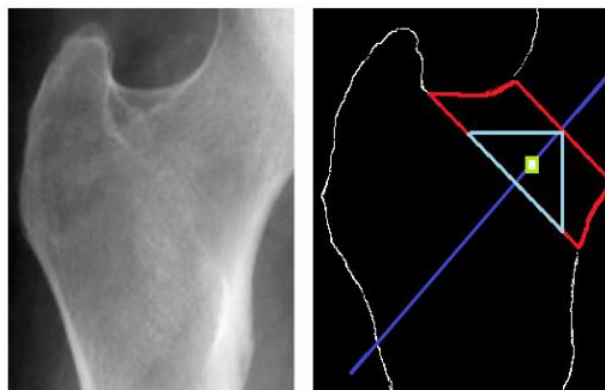


Fig.3 Regions of interest in the head of the femur

2.1 Obtaining the image

In the initial instance, the radiologist obtains the radiographic sheets and stores the radiological image in digital form using the digital features of the healthcare equipment or through a capture device. For this project, a Radlink Laser Pro 16 medical image scanner was used, which has resolution capabilities of up to 6 pixels per millimetre.

2.2 Delimitation of areas of interest

In this case, the regions of interest correspond to the areas of the image that contain the information required for the subsequent stages of processing, removing the unnecessary data from the original data volume. The management of the images is done in three levels: the full image, the delineation of a region of interest, as well as the detection of the regions of interest. This is done to preserve environmental data. The area of interest within the image must be delimited in this manner after the image has been acquired. The head as well as the neck attached to the femur are located in this region for hip images like those used in this work. Delimitation is carried out manually.

2.3 Pre-Processing Tasks

In terms of the computation itself, methods for reducing noise or principles that don't help reveal information about the trabecular structure are first applied. The primary goal of the methods used in this study is oriented toward choosing of the region of interest (TW, GCP), even though the project is working on the creation of noise reduction methods to achieve the decrease in soft tissue contribution and be able to bring out more trabecular information. The use of smoothing methods or lower-pass filtering is one way to lessen noise. The analysis of the behavior of a group of methods for noise reduction is one of the work subjects of the project described in the section Context.

2.4 Segmentation

The application of edge detection techniques can be used to solve the zone segmentation problem in the image. The contours are very helpful for segmenting and identifying objects in scenes because they describe the borders of the objects. In this work, it is suggested that edge detection methods be used to identify the bone's contour. In order to choose the edge operator that yields the best results, various edge operators [20] (Sobel, Prewitt, Frei-Chen, Roberts, custom filters) are being researched. The resulting image is binarized using algorithms like Otsu [21] in order to categorize the pixels according to their edge characteristics. It implies thinning, which is one of the issues with detecting an irregular contour like the edge of the femur bone. Techniques like erosion and dilation are used for this. Erosion happens when marginal pixels change their logical value from 1 to 0. The search for marginal pixels with logical value 1 who have a neighbour with logical value 0 constitutes the criteria to apply erosion. By using a similar dilation criterion, we search for pixels that are close to the object's marginal line and change their logical value from 0 to 1. The erosion process results in a reduction in the image's area, while the dilation process results in an increase. When erosion is applied after dilation (the opposite of opening), an image is said to be locked. Filling in the blanks and joining things that are near one another define this process.

2.5 Binary Image

The input image becomes a binary image after the procedures described above are completed. The pixels at 1 most external to the matrix will be the edges of our image. To accomplish this, we will look at each pixel's neighbors to determine whether or not the pixel we are processing is an edge pixel. The group of empty pixels with at least four black neighbors forms the edge of the white image.

2.6 Determine the Contour of the Femur

The edges of the femur must be formed by a single pixel in order to obtain the contour of the femur in the image. In order to achieve this, the idea of "skeletonization" is applied, which aims to produce from an image a continuous pattern with the least amount of data possible while retaining a trace of the original object. There are algorithms for this that function generally, removing pixels in accordance with pre-established rules, and stopping when there are no more changes to be made.

The Hildich algorithm is suggested [22]. It's possible that some of the pixels in the image don't contain any information in addition to displaying the bone's contour. To achieve this, a technique is used in which the maximum amount of data that does not contain information pertinent to the issue is eliminated. The basic idea is to create a single path that runs from the top of the image to the bottom, forming the left contour of the femur.

2.7 Determine the TW Later

We continued our search for Ward's triangle from the femur bone skeleton image (Fig. 3). This process entails a number of geometric steps, which are described below:

- Find the line that is furthest away from the femur's neck (the slightest red line in Fig. 3).
 - Determine the axis of symmetry for the given line (based on the slope and midpoint of the line of minimum distance; see Fig. 3, blue line).
 - Locate the critical point, which was determined by approximating tangents with straight lines that were 5 points long.
 - Locate the base line that passes through the critical point and is perpendicular to the axis (see Fig. 3, a long red line).
- and. Find the triangle (light blue in Fig. 3): A) Locate the intersection of the minimum distance line. B)

Locate the intersection of the perpendicular lines that pass the two extreme points of the line of minimum distance, as well as the line (base of the triangle) whose points belong to the base line.

E. Form the triangle with the data obtained in A) and B).

F. Find the central point of the triangle (see Fig. 3, in blue) and define a square of $N \times N$ centered on this point which is called "Ward Triangle" (see Fig. 3, in green).

IV. RESULTS OBTAINED

According to preliminary findings, a subset of carefully chosen images had the Ward triangle automatically detected using image processing methods. Applying these techniques should yield results that are comparable for the Main Compressive Group, giving rise to a tool that can be used to choose the study areas for osteoporosis diagnosis.

In Fig. 4, the area of interest is manually delineated in 2a, the edge operator image is shown in 2b, the binarization image is shown in 2c, the erosion technique image is shown in 2d, and the residual branches of the erosion are removed in 2e. These successive results of the application of the algorithm presented in this work can be seen.

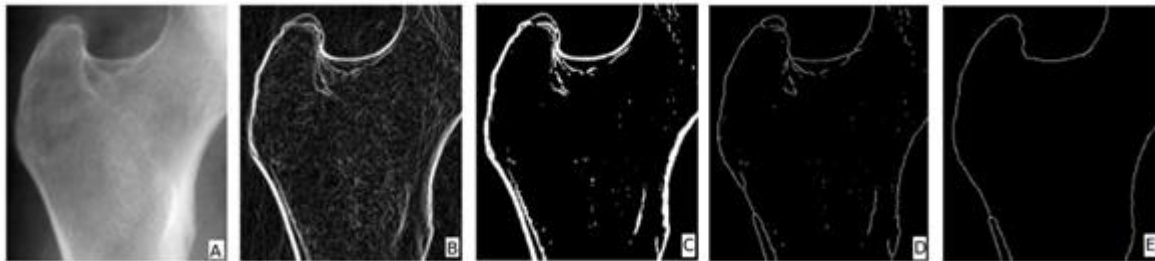


Fig.4 Results of each of the stages proposed

V. CLASSIFICATION

We developed a two-level classification model using all the radiomic features available to classify the bone density status of each VB as normal, osteopenia, or osteoporosis. This model included two support vector machine (SVM) binary classifiers for the hierarchical binary classification of each patient's bone density status (normal vs. abnormal; if abnormal, osteopenia vs. osteoporosis). Then, in the training phase, we defined the nested cross-validation (CV) scheme with four outer and four inner iterations. At each iteration, data were divided into a training set and a test set. To further refine the model's hyperparameters using a Bayesian approach, we used a second round of fivefold CV to divide the training set into an inner training set and a validation set.; This method allows for the optimization of models without the alleged information leakage from the hold-out (outer) set of tests. The validation set's sensitivity, specificity, accuracy, and area under the receiver's operating curves (AUC) were all determined after the model was developed. Using the hyperparameters selected during the inner CV iterations, the model was trained on all of the training data for the outer CV rounds. The final performance level of our SVM model was determined using the test set and average metrics across four outer creases (each with 100 repetitions), and feature ranking was carried out using feature weights from the instructed SVM model with a linear kernel [23].

VI. FINITE ELEMENT METHOD

With the help of this technique, models can be optimized without worrying about alleged information leakage from the hold-out (outer) set of tests. After the model was created, the sensitivity, specificity, accuracy, and area under the receiver's operating curves (AUC) of the validation set were all determined. The model was trained on all of the training data for the outer CV rounds using the hyperparameters chosen during the inner CV iterations. The test set and average metrics across four outer creases (each with 100 repetitions) were used to determine the final performance level of our SVM model, and feature ranking was carried out using feature weights from the instructed SVM model with a linear kernel [23].

Silva et al. found that in healthy subjects, the cortical shell is unable to support a significant amount of the load at the spine [24]. According to claims made in comparison to estimates of strength derived from voxel-based finite element models, clinical measures of bone density obtained from QCT, regardless of bone size, are less reliable indicators of in vitro vertebral compressive strength [25]. This benefit of FEM might not be applicable if more intricate parameters other than just mid-vertebral trabecular BMD and bone size are measured [26].

Cross-sectional studies using clinical CT scans do not require imaging recovery for FEM, but longitudinal studies that aim to track more subtle changes in rigidity over time should consider the tiny but very significant effects of voxel size [27,28].

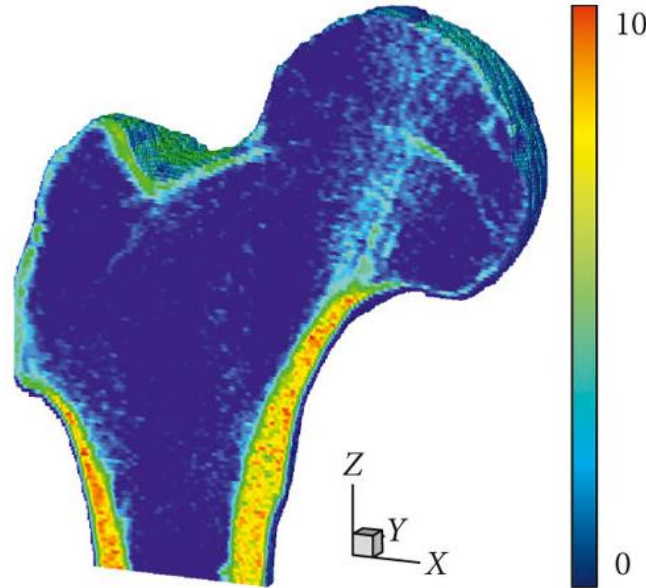


Fig.5 Distribution of Young's modulus computed from BMD

VII. CHALLENGES WITH BONE IMAGING

Developed bone visualization for osteoporosis assessment has come a long way in the past 20 years, but there are still many challenges to be solved. Technically, the challenges stem from trade-offs and compromises between spatial resolution, sample size, signal-to-noise, radiation exposure, and acquisition time, or between the complexity and expense of imaging technologies in comparison to their accessibility and availability.

The challenges of bone imaging in clinical practice include balancing the advantages of standard BMD data with the more complex bone building features or the laboratory's need for in-depth research with the more general requirements of clinical practice. The biological differences between the central axial structure and the peripheral appendicular bones, as well as how they affect the most suitable bone imaging techniques, must be made clear. The relative merits of these cutting-edge imaging methods must also be contrasted between their applications as monitoring processes, which demand high precision or reproducibility, and their applications as medical diagnostics, which demand high accuracy or reliability.

VIII. CONCLUSION

The project's primary goal is the development of texturing characterization methods, in this case trabecular textures, which enable the creation of indices that measure the quality of various tissues and link them to diagnostic markers in order to discover relationships between them.

The quality of conventional methods can be raised by combining them with indexes gleaned from diagnostic assistance tools. It has recently been acknowledged that using image analysis techniques to describe the trabecular structure of bone can be useful in the diagnosis of osteoporosis.

REFERENCES

- [1]. Kanis JA, McCloskey EV, Johansson H, Cooper C, Rizzoli R, Reginster JY. European guidance for the diagnosis and management of osteoporosis in postmenopausal women. *Osteoporos Int* 2013;24:23-57.
- [2]. Dougherty G. *Digital Image Processing for Medical Applications*, Cambridge University Press, 1 edition, 2009.
- [3]. Martinez, Viglietti, "Tool for Vector Analysis of Trabecular Textures in Osteoporosis". Thesis of the Degree in Systems Engineering, Tandil, 2009.

- [4]. Pecelis, Massa, Favro Velo, Santiago, Caselli, "Classification of trabecular patterns in the proximal femur using the vector representation algorithm: its correlation to the degree of osteoporosis", WC, 2009.
- [5]. Guglielmi G, Muscarella S, Bazzocchi A. Integrated imaging approach to osteoporosis: state-of-the-art review and update. *Radiographics* 2011;31:1343-64.
- [6]. Engelke K, Glüer CC. Quality and performance measures in bone densitometry. *Osteoporos Int* 2006;17:1283-92.
- [7]. Oei L, Koromani F, Rivadeneira F, Zillikens MC, Oei EH. Quantitative imaging methods in osteoporosis. *Quant Imaging Med Surg* 2016;6:680-98.
- [8]. Stone KL, Seeley DG, Lui LY, Cauley JA, Ensrud K, Browner WS, Nevitt MC, Cummings SR, Osteoporotic Fractures Research Group. BMD at multiple sites and risk of fracture of multiple types: long-term results from the Study of Osteoporotic Fractures. *J Bone Miner Res* 2003;18:1947-54.
- [9]. Reproduced from *J Bone Miner Res* 1986; 1:16–21 with permission from American Society for Bone and Mineral.
- [10]. Adams JE. Advances in bone imaging for osteoporosis. *Nat Rev Endocrinol* 2013;9:28-42.
- [11]. Adams JE. Advances in bone imaging for osteoporosis. *Nat Rev Endocrinol* 2013;9:28-42.
- [12]. Bandirali M, Lanza E, Messina C, Sconfienza LM, Brambilla R, Maurizio R, Marchelli D, Piodi LP, Di Leo G, Ulivieri FM, Sardanelli F. Dose absorption in lumbar and femoral dual energy X-ray absorptiometry examinations using three different scan modalities: an anthropomorphic phantom study. *J Clin Densitom* 2013;16:279-82.
- [13]. Marshall D, Johnell O, Wedel H. Meta-analysis of how well measures of bone mineral density predict occurrence of osteoporotic fractures. *BMJ* 1996;312:1254-9.
- [14]. Bandirali M, Poloni A, Sconfienza LM, Messina C, Papini GD, Petrini M, Ulivieri FM, Di Leo G, Sardanelli F. Short-term precision assessment of trabecular bone score and bone mineral density using dual-energy X-ray absorptiometry with different scan modes: an in vivo study. *Eur Radiol* 2015;25:2194-8.
- [15]. Delnevo A, Bandirali M, Di Leo G, Messina C, Sconfienza LM, Aliprandi A, Ulivieri FM, Sardanelli F. Differences among array, fast array, and high-definition scan modes in bone mineral density measurement at dual-energy x-ray absorptiometry on a phantom. *Clin Radiol* 2013;68:616-9.
- [16]. Messina C, Bandirali M, Sconfienza LM, D'Alonzo NK, Di Leo G, Papini GDE, Ulivieri FM, Sardanelli F. Prevalence and type of errors in dual-energy x-ray absorptiometry. *Eur Radiol* 2015;25:1504-11.
- [17]. Bachrach LK. Assessing bone health in children: who to test and what does it mean? *Pediatr Endocrinol Rev* 2005;2 Suppl 3:332-6.
- [18]. Wasserman H, Gordon CM. Bone Mineralization and Fracture Risk Assessment in the Pediatric Population. *J Clin Densitom* 2017;20:389-96.
- [19]. J. R. Zanchetta, J. R. Talbot, Osteoporosis, "Osteoporosis: physiopathology, diagnosis, prevention and treatment". Buenos Aires: Medica Panamericana, 2001.
- [20]. Tinku Acharya, Ajoy K. Ray, "Image Processing principles and applications", Hardcover, Sept. 8, 2005.
- [21]. Otsu, Nobuyuki, "A thresholding selection method from gray-level histogram", *IEEE Transactions on Systems*, Volume 17, Issue 3, p. 279-284, 1984.
- [22]. Nabil Jean Naccache and Rajjan Shinghal, "An investigation into the skeletonization approach of hilditch", 1984.
- [23]. Roski F, Hammel J, Mei K et al (2019) Bone mineral density measurements derived from dual-layer spectral CT enable opportunistic screening for osteoporosis. *Eur Radiol* 29:6355–6363
- [24]. body compressive strength better than quantitative computed tomography: an examination of stress-and strain-based failure theories. *J Biomech* 2000;33: 209–14.
- [25]. SilvaMJ, KeavenyTM, HayesWC. Load sharing between the shell and centrum in the lumbar vertebral body. *Spine* 1997;22:140–50.
- [26]. CrawfordRP, Cann CE, Keaveny TM. Finite Element Models Predict In Vitro Vertebral body compressive strength better than quantitative computed tomography. *Bone* 2003;33:744–50.
- [27]. MastmeyerA, EngelkeK, FuchsC, KalenderWA. A hierarchical 3D segmentation method and the definition of vertebral body coordinate systems for QCT of the lumbar spine. *Med Image Anal* 2006;10:560.
- [28]. CrawfordRP, RosenbergWS, KeavenyTM. Quantitative computed tomography based finite element models of the human lumbar vertebral body :effect to element size on stiffness, damage, and fracture strength predictions. *J BiomechEng* 2003;125:434–8.